ELSEVIER

PII: S0032-3861(97)00218-8

Polymer Vol. 39 No. 1, pp. 99–107, 1998

0032-3861/97/$17.00+0.00

Rheology and morphology of compatibilized polyamide 6 blends containing liquid crystalline copolyesters

Y. Z. Meng* and S. C. Tjong†
Department of Physics and Materials Science, City University of Hong Kong, Tat Chee Avenue, Kowloon, Hong Kong
(Received 21 November 1996; revised 17 January 1997)

The rheology, mechanical properties and microstructural development during capillary flow of maleic anhydride compatibilized polyamide 6 [PA6(MAP)] blends containing liquid crystalline polymers (LCPs) were studied by means of the capillary rheometer, tensile test and scanning electron microscopy (SEM). The LCPs used were Vectra A950, and a copolyester consisting of 60 mole percent p-hydroxybenzoic acid (PHB) and 40 mole percent poly(ethyleneterephthalate) (PET). The rheological measurements showed that the viscosity ratio between the Vectra A950 and [PA6(MAP)] matrix is much larger than unity. This implied that the LCP fibrillation is unlikely to occur in the [PA6(MAP)] blends containing Vectra A950 additions. However, SEM observations revealed that long and fine fibrils are formed extensively in the matrix of [PA6(MAP)] polyblends containing Vectra A950 content $\geq$ 20 wt%. Consequently, the tensile strength of these polyblends appeared to increase with increasing LCP content, and deviated from the predictions of the rule of mixtures. On the other hand, the viscosity ratio between the 60/40 PHB/PET and [PA6(MAP)] matrix is smaller than unity, thus favouring the formation of LCP fibrils. But, the SEM examinations showed that the LCP phase dispersed into porous and foamy structure in the matrix owing to the decomposition of 60/40 PHB/PET polymer and PA6(MAP) during processing. In this case, the tensile strength of the [PA6(MAP)] polyblends containing 60/40 PHB/PET polymer appeared to decrease sharply with increasing LCP content. The correlation between the flow properties and LCP morphology was discussed. © 1997 Elsevier Science Ltd.

(Keywords: viscosity; fibrillation; polyamides)

INTRODUCTION

Recently, polyblends containing thermotropic liquid crystalline polymers (LCPs) and thermoplastics have attracted much research attention[1–8]. The interest arises from two major advantages of blending LCPs with engineering thermoplastics. First, the LCPs can exhibit low melt viscosity, hence the addition of a small amount of LCPs to thermoplastics can result in a considerable reduction in the blend melt viscosity thereby improving the processability of engineering plastics. Second, the LCPs have a more rigid molecular structure and they generally exhibit a high degree of order in the melt under the conditions of shear and extension during processing. Therefore, the LCP phase can deform into fibrillar domains, and these fibrils than act as the reinforcing element in the in situ composite as a result of the inherent high strength and stiffness of the LCPs. The fibrillation of LCP in thermoplastic melts is influenced by several factors. These include miscibility between the LCP and thermoplastics, LCP concentration, and processing parameters such as the melt viscosity ratio of LCP to polymer matrix (V_r) melt temperature, flow mode and shear rate.

Most LCP/thermoplastic blends are composed of immiscible or partly miscible polymers. Immiscible polymer blends are characterized by a two-phase morphology and poor chemical/physical interactions across the phase boundaries. The poor interfacial adhesion between the LCP domains and polymer matrix leads to the polyblends having low tensile strength and modulus. In order to induce compatibility between LCP and thermoplastics, graft polymers or copolymers have been introduced in LCP/thermoplastic systems. For example, Baird and co-workers have studied the effect of maleic anhydride grafted polypropylene (MAP) on the morphology and mechanical properties of PP/LCP blends[9–12]. They reported that the adhesion between the LCP and polymer matrix is greatly improved by the presence of MAP which acts as an effective compatibilizer. The MAP does not directly react with the LCP. Instead, hydrogen bonding is believed to be responsible for the compatibilizing effect. Moreover, the MAP addition leads to a finer and more uniform distribution of the LCP phase in polypropylene (PP). Consequently, significant enhancements in both tensile modulus and strength are achieved in the PP/LCP blends[12]. Wei *et al.*[13] have developed a compatibilizer based upon the transesterification between the polycarbonate (PC) matrix and a second LCP that contains the same liquid-crystalline chemical structure as that in the reinforcing LCP. Therefore, the compatibilizer is a block copolymer exhibiting crystalline character. In this case, a physical interaction exists between the matrix polymer and LCP through the compatibilizer. Thus, the compatibilized PC/LCP blends display improved ultimate tensile strength, elongation at break and impact properties[13].

* Y. Z. Meng is on leave from the Department of Polymer Science and Materials, Dalian University of Technology, Dalian, China.
† To whom correspondence should be addressed.

Several researchers have studied the flow behaviour of LCP/thermoplastic blends[14–18]. It is commonly observed that the LCP fibrillation occurs when the viscosity ratio of LCP to polymer matrix is smaller than or near to unity. Beery *et al.*[14] have investigated the structure development during capillary flow of polyblends containing LCP. The thermoplastics used were poly(butylene terephthalate) (PBT), PC and polyamide 6 (PA 6). They indicated that fine fibrils are developed in the PC/LCP system where the viscosity of the matrix is higher than that of the LCP. In cases where the viscosity of the matrix was lower than the LCP phase (PA6), fibrous structure develops only at very high shear rates. In another study, Subramanian and Isayev showed that LCP fibrillation does not occur in the matrix of poly(phenylene sulfide) (PPS) because the viscosity of PPS is lower than that of the LCP[19]. They further examined the fibril formation in the blends of polyether ether ketone (PEEK) with LCP where the LCP has a higher shear viscosity at the processing temperature than the thermoplastic polymer[20]. The results of investigation showed that the LCP ellipsoids develop in the matrix of PEEK at low LCP concentration. Furthermore, extended ellipsoids can be observed at 25 wt% LCP composition. At higher LCP concentration (50 wt%), phase inversion is noticeable in the blend with the formation of PEEK fibrils in the matrix of LCP[20]. In addition to the viscosity ratio of the component polymers, LCP fibrillation is generally favoured under elongational conditions such as those prevailing at the entrance of the extrusion die and during the subsequent drawing of the extrudate. This is because extensional flow field is more effective at elongating the droplets into fibrils than the shearing flow. In injection moulding, a skin-core structure usually develops in the moulded parts where highly oriented molecules are only found in the skin layer. The high degree orientation results from the extensional flow at the advancing flow front and rapid cooling near the mould surface[8]. Finally, it is recognized that the processing temperature of the LCP/thermoplastic blends must be carefully selected. Blends prepared at temperatures near the LCP solid to nematic transition generally exhibit higher mechanical properties than systems fabricated at significantly higher temperatures. This is due to the disintegration of LCP fibrils into droplets at higher processing temperatures.

In previous work, we have investigated the morphology and mechanical properties of the injection moulded PA6/LCP blends compatibilized with MAP, i.e. PA6(MAP)/LCP blends[21,22]. The results showed that the processing steps and temperatures have a dramatic effect on the fibrillation of LCP in the compatibilized PA6/LCP blends. LCP fibrillation does not take place in PA6(MAP)/LCP blend at 295°C due to the thermal degradation of PA6[21]. However, it is observed that one-step injection moulding of PA6(MAP) with LCP pellets at 285°C facilitates fibrillation of LCP phase in the PA6(MAP)/LCP blends[22]. This paper represents a continuation of our studies on the effect of MAP compatibilization on the LCP fibrillation in PA6 blends. Two kinds of LCPs are used in this work. The first LCP is a wholly aromatic copolymer consisting of 27 mole percent 2,6-hydroxynaphthoic acid (HNA) and 73 mole percent p-hydroxybenzoic acid. The second LCP is a copolyester consisting of 60 mole percent p-hydroxybenzoic acid (PHB) and 40 mole percent poly(ethylene terephthalate) (PET). The aim of this paper is to study the rheological behaviour of the PA6(MAP)/LCP blends and to determine the correlation between the flow behaviour with the structural and mechanical properties of the blends.

EXPERIMENTAL

Materials

The LCPs used in this work are Vectra A950 produced by Hoechst Celanese company, and the copolyester of 60 mole percent p-hydroxybenzoic acid (PHB) and 40 mole percent poly(ethylene terephthalate) (PET) supplied by Beijing Chemical Research Institute (China). The former copolyester is designated as LCP_1 whereas the latter is designated as LCP_2 in this work. The glass transition and melting temperatures of Vectra A950 (LCP_1) are 105 and 283°C, respectively. Russian made PA6 pellets (PA6-120/321) are used as the matrix material. The PP is a commercial product of Himont (Profax 6331) with a melt flow index of 12 g/10 min. The maleic anhydride (MA) supplied by Fluka Chemie and the dicumyl peroxide (DCP) produced by Aldrich Chemical Company are used for the maleation of PP. The PA6, PP and LCP pellets were dried in an oven at 100°C for 24 h prior to blending.

Blending procedure

The maleated PP (MAP) was prepared in a twin-screw Brabender Plasticorder at 220°C and 15 rpm by one-step reaction of PP with MA in the presence of DCP. The weight ratio of PP, MA and DCP was fixed at 94:6:0.3. The extrudates were cut into pellets by a pelletizer. Then, the 86 wt% PA6 and 14 wt% MAP were mixed at 260°C. The extrudates were also pelletized upon exiting the extruder. This binary blend was used as the matrix material, and it was designated as PA6(MAP) throughout this paper. Dog-bone shaped tensile bars (ASTM D-638) were injection moulded from the PA6(MAP) pellets.

The PA6(MAP)/LCP_1 and PA6(MAP)LCP_2 polyblends were also prepared in Brabender at 280°C and 240°C, respectively. The extrudates were again granulized. The LCP contents were 0, 5, 10, 15, 20, 25, 30 and 40 wt% for the PA6(MAP/LCP_1 and PA6(MAP)/LCP_2 polyblends. Standard dog bone tensile bars were injection moulded from the pellets of these polyblends. The mould temperature was maintained at 40°C. The barrel zone temperatures were set at 270-285-285°C and 235-240-240°C for PA6(MAP)/LCP_1 and PA6(MAP)/LCP_2 polyblends, respectively.

Static mechanical properties

The tensile behaviour of the specimens were determined using an Instron tensile tester (model 4206) at 23°C with a relative humidity of 50%. A crosshead speed of 1 mm/min was used in the measurements. The gauge length of the specimens was 57 mm. Five specimens of each composition was tested and the average values reported.

Morphology observation

The morphologies of the fracture surfaces of all polyblends were observed in a scanning electric microscope (SEM; JEOL JSM 820). The specimens were fractured in liquid nitrogen and the fracture surfaces were coated with a thin layer of gold prior to SEM examinations.

Differential scanning calorimetry (DSC)

DSC measurements were carried out using an Perkin–Elmer calorimeter (model DSC-7) from 30 to 350°C at a heating rate of 10°C/min under a protective nitrogen atmosphere.

Rheological measurements

Rheological properties of the polybleds and pure polymers were measured using a Rheograph capillary rheometer (model 2003). The capillary had 1 mm diameter and 30 mm long (L/D = 30). The Rabinowitch correction was applied to all experimental data, whereas the entrance effect was neglected due to high L/D ratio. The shear range investigated was within 20–6000 s^{-1}. The extruded strands produced from the rheometer were quenched into a cold water bath.

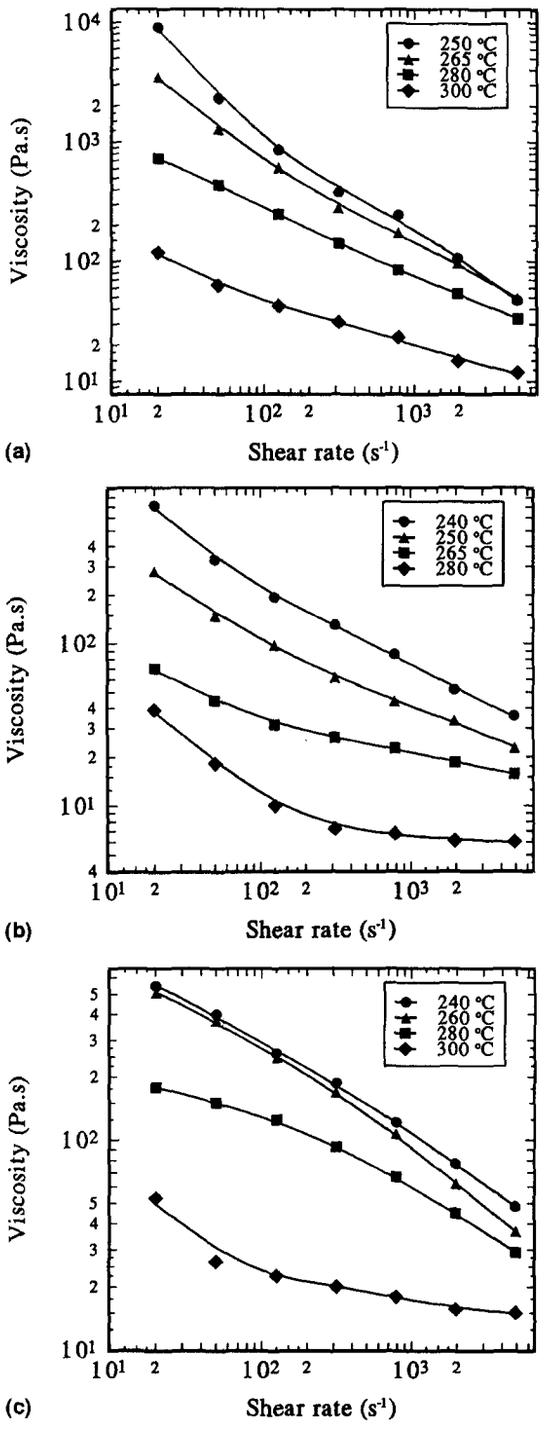

Figure 1 Viscosity vs shear rate for (a) LCP_1, (b) LCP_2 and (c) PA6(MAP) matrix at various temperatures

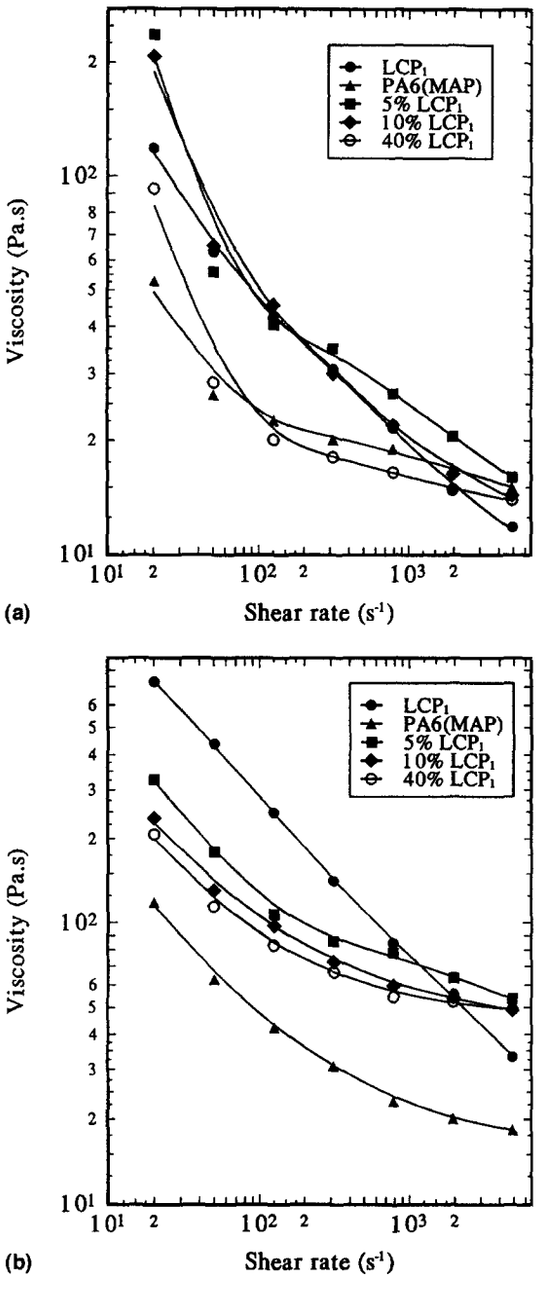

Figure 2 Viscosity vs shear rate for PA6(MAP)/LCP_1 system at (a) 300 and (b) 280°C

Table 1 Values of viscosity ratio between the LCP_1 and the PA6(MAP) matrix extruded at various shear rates

	Shear rate (s^{-1})						
Temperature (°C)	20.04	50.00	125.00	312.50	781.30	1953	4883
300	2.24	2.39	1.87	1.54	1.14	0.87	0.79
280	6.14	6.96	5.86	4.57	3.67	2.76	1.81

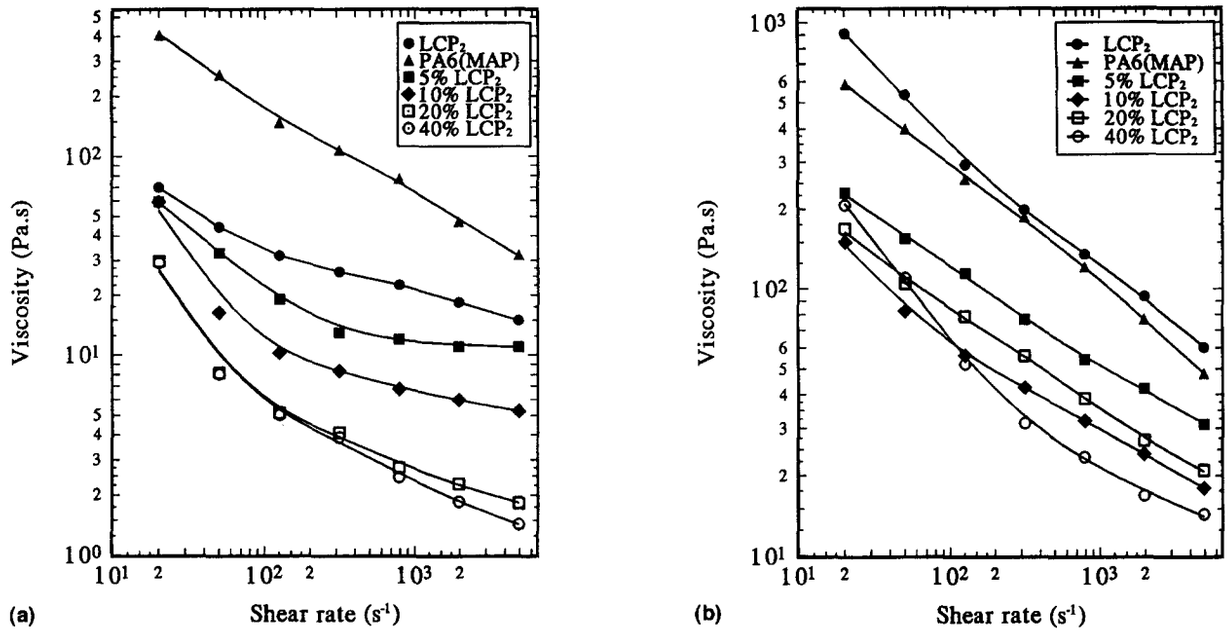

Figure 3 Viscosity vs shear rate for PA6(MAP)/LCP_2 system at (a) 265 and (b) 235°C

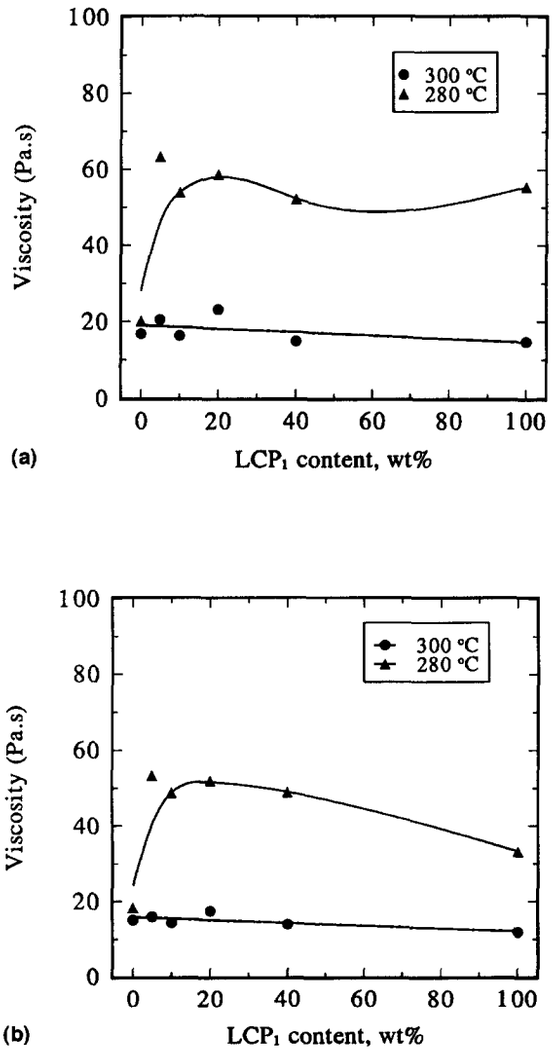

Figure 4 Viscosity vs LCP content for PA6(MAP)/LCP_1 system at a shear rate of (a) 1953 and (b) 4883 s^{-1}

RESULTS AND DISCUSSION

Rheological behaviour

Figure 1a–c show the viscosity vs shear rate data for the LCP_1, LCP_2 and PA6(MAP) matrix at various temperatures. Apparently, the LCPs and the matrix in the studied range of shear rates exhibit a non-Newtonian flow behaviour. The viscosity of LCP_1 decreases with increasing temperature from 250 to 300°C. The LCP_1 viscosity changes much less between 250 and 265°C than that between 280 and 300°C. At temperatures of 280°C and above, the viscosity of the LCP_1 is higher than that of the PA6(MAP) matrix. The viscosity of the LCP_2 also decreases with increasing temperatures from 240 to 280°C and it is too low to be measured at 300°C. It is noticed that the viscosities of LCP_1 and LCP_2 decrease sharply with increasing shear rate. *Figure 2a* shows the viscosity curves measured for the PA6(MAP)/LCP_1 blend system at 300°C. The LCP_1 exhibits a monotonical shear thinning behaviour over the entire range of shear rates investigated. The viscosity of the LCP_1 is higher than that of the PA6(MAP) matrix at low and intermediate shear rate range but it reverses at the crossover point. At this point, i.e. a shear rate of about 2000 s^{-1}, the flow curves of the LCP_1 and the PA6(MAP) matrix intersect. This means that the viscosity ratio of the LCP to polymer matrix (V_r) is smaller than unity when the shear rate is above the crossover point. The crossover point has practical significance as maximum fibrillation occurs at this point[16]. At 280°C, the flow curves of the LCP_1 and the PA6(MAP) matrix does not intersect, and the viscosity of the LCP_1 is much higher than the matrix in the entire shear range studied. Moreover, the viscosities of the blends are intermediate between the neat LCP_1 and the matrix (*Figure 2b*). *Figure 3a* and *b* show the flow curves of the LCP_2, PA6(MAP) and PA6(MAP)/LCP_2 system extruded at 265 and 235°C. It is evident from *Figure 3a* that the viscosity of the LCP_2 is considerably lower than that of the PA6(MAP) matrix in entire shear rate range studied at 265°C. The viscosities of the PA6(MAP)/LCP_2 blends are lower than those of parent polymers, and they appear to decrease dramatically with

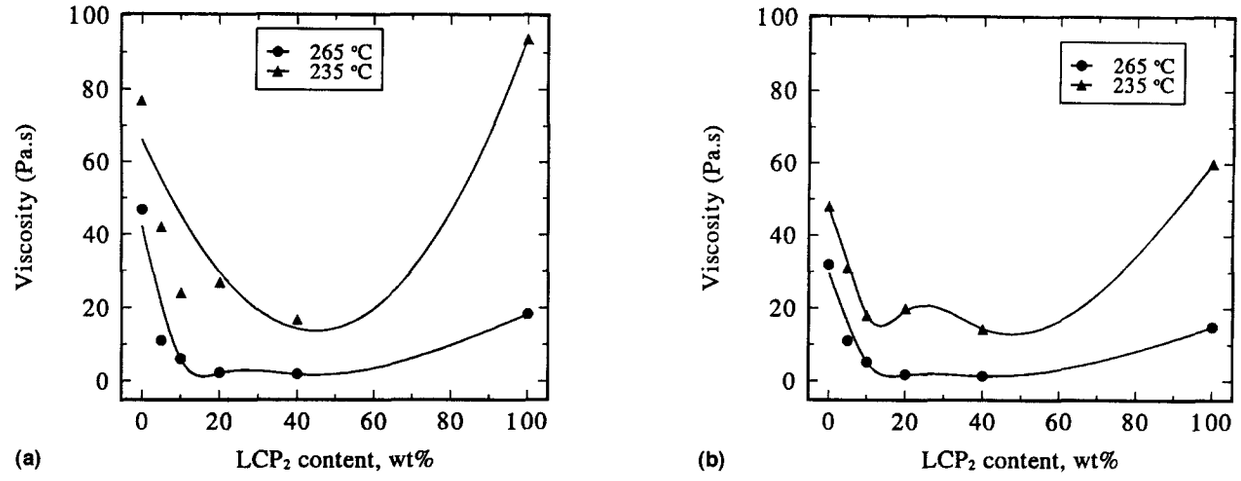

Figure 5 Viscosity vs LCP content for PA6(MAP)/LCP_2 system at a shear rate of (a) 1953 and (b) 4883 s^{-1}

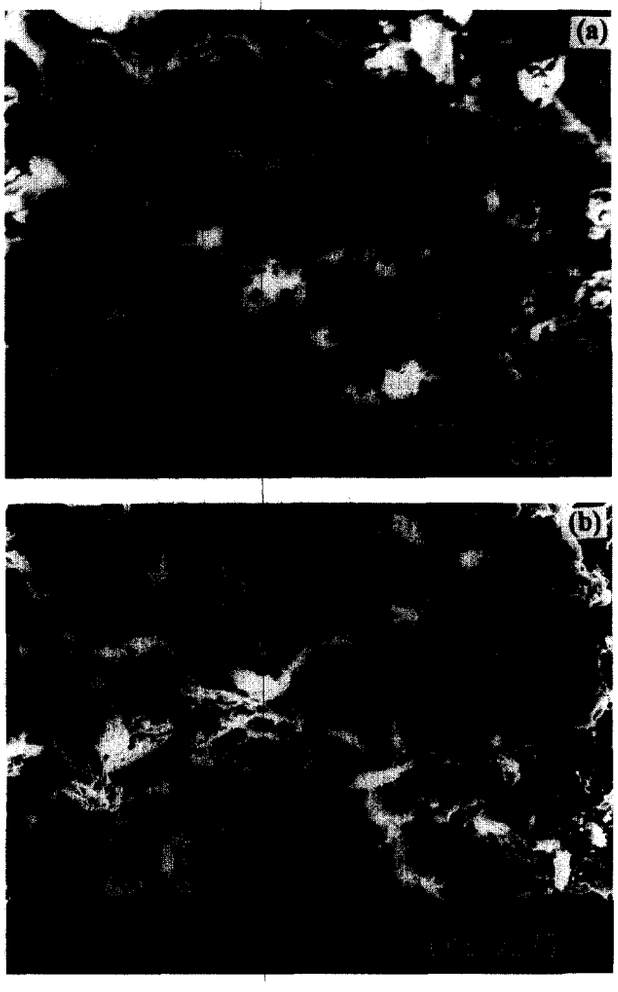

Figure 6 SEM micrographs of the PA6(MAP)/5% LCP_1 blend extruded at (a) 300 and (b) 280°C under a shear rate of 4883 s^{-1}

increasing LCP_2 content. The values of the viscosity ratio between the LCPs and PA6(MAP) matrix at various shear rates are summarized in *Table 1* and *Table 2*. *Table 1* reveals that the rheological properties of PA6(MAP) and LCP_1 are unfavorable for the formation of LCP fibrils at 280°C in the range of shear rates studied due to the V_r values are larger than one. LCP fibrillation only likely occurs in the PA6(MAP)/LCP_1 system at 300°C and at shear rates approach 1953 s^{-1} and above. On the other hand, *Table 2* shows that the viscosity ratios of LCP_2 to PA6(MAP) matrix is smaller than one thereby favouring the formation of LCP fibrils. However, the V_r values listed in *Tables 1 and 2* do not correlate well with the LCP morphology of the PA6(MAP)LCP blends as observed by SEM. The reason for this will be discussed later.

Figure 4a–b show the plots of viscosity vs LCP content for the PA6(MAP)/LCP_1 blend system at shear rate of 1953 and 4883 s^{-1}, respectively. From *Figure 4a*, the viscosity of the neat LCP_1 extruded at 300°C is slightly smaller than that of the PA6(MAP) matrix. The addition of LCP results in a decrease in melt viscosity of the PA6(MAP)/LCP_1 blends. On contrary, the melt viscosity of LCP_1 is higher than that of the matrix at 280°C, hence the viscosity of the PA6(MAP)LCP_1 blends appears to increase with increasing LCP_1 content. Therefore, the PA6(MAP)/LCP_1 blends have their flow properties affected by the presence of LCP_1. A similar flow behaviour is observed for the PA6(MAP)/LCP_1 blend system extruded at a shear rate of 4883 s^{-1} (*Figure 4b*). For the PA6(MAP)/LCP_2 blends, the viscosity of the LCP_2 is higher than that of the matrix extruded at 235°C under a shear rate of 1953 s^{-1}. But the viscosity of the PA6(MAP)/LCP_2 blends tends to decrease with increasing LCP_2 content and an apparent minimum was observed in this blend system containing 40 wt% LCP_2 (*Figure 5a*). In addition, this figure also indicates that the blend viscosity also appears to decrease with increasing LCP_2 content at 265°C owing to the LCP_2 exhibits a lower

Table 2 Values of viscosity ratio between the LCP_2 and the PA6(MAP) matrix extruded at various shear rates

	Shear rate (s^{-1})						
Temperature (°C)	20.04	50.00	125.00	312.50	781.30	1953	4883
265	0.17	0.17	0.21	0.24	0.29	0.39	0.47
235	1.55	1.34	1.13	1.07	1.11	1.22	1.25

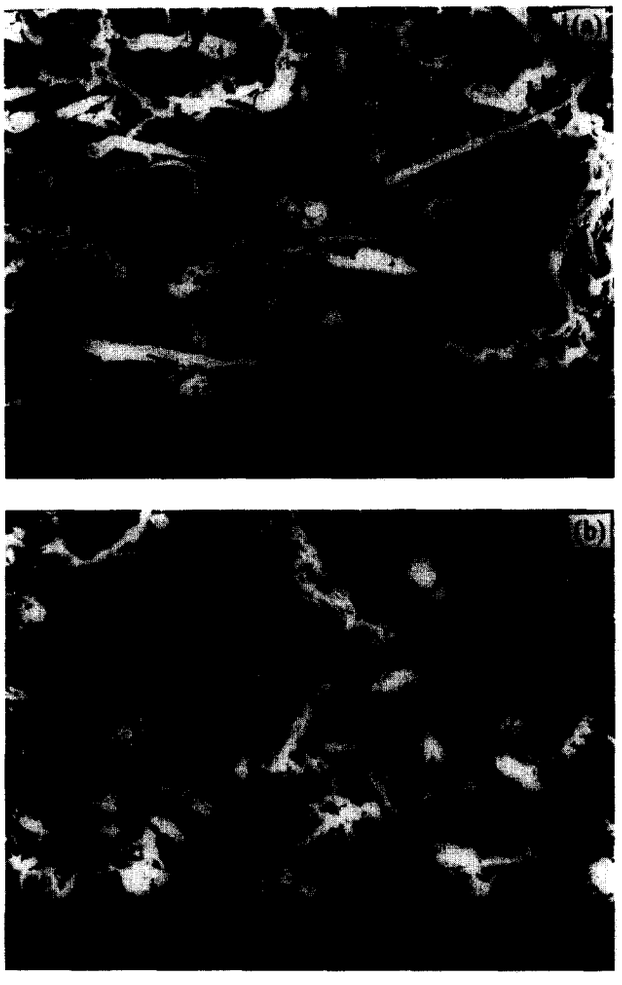

Figure 7 SEM micrographs of the PA6(MAP)/10% LCP_1 blend extruded at 280°C under a shear rate of (a) 4883 and (b) 50 s^{-1}

melt viscosity than that of the PA6(MAP) polymer. *Figure 5b* shows the variation of melt viscosity with LCP content for the PA6(MAP)/LCP_2 blends extruded at a shear rate of 4883 s^{-1}. It is noticed that the incorporation of LCP_2 also lowers the melt viscosity of PA6(MAP)/LCP_2 blends. For the PA6(MAP)/LCP_2 blend system, it can be concluded that the blend viscosity always decreases with increasing LCP_2 content whether the viscosity of LCP_2 is higher or lower than that of the PA6(MAP) polymer.

Blend morphology

Figure 6a and *b* show typical SEM micrographs of the PA6(MAP)/5%LCP_1 blend subjected to a high shear rate of 4883 s^{-1} at 300 and 280°C, respectively. It can be seen that the LCP dispersed as coarse ellipsoids in the matrix of the PA6(MAP)5%LCP_1 blend. Only few cavities can be discerned in these micrographs indicating the compatibility between the LCP_1 and polymer matrix is improved by the incorporation of MAP into the blend. Increasing the LCP_1 content to 10 wt.% leads to the formation of fine LCP fibrils in polymer matrix (*Figure 7a*). However, it is evident that only elongated ellipsoids are developed in the matrix of PA6(MAP)/10%LCP_1 blend subjected to a low shear rate of 50 s^{-1} (*Figure 7b*). Thus, the development of LCP microfibrils in polyblends depends significantly on the shear rates and LCP content. *Figure 8a–b* show the SEM fractographs of the PA6(MAP)20%LCP_1 blend subjected to a low shear rate of 50 s^{-1} at 300 and 280°C,

Figure 8 SEM micrographs of the PA6(MAP)/20% LCP_1 blend extruded at (a) 300 and (b) 280°C under a shear rate of 50 s^{-1}; (c) SEM micrograph of the PA6(MAP)20% LCP_1 blend extruded at 280°C under a shear rate of 4883 s^{-1}. This photograph is taken from the blend broken in liquid nitrogen parallel to the flow direction

respectively. The microstructure of this polyblends extruded at both temperatures is characterized by the formation of both fine and coarse fibrils. At high shear rate extended fine fibrils are formed extensively in the PA6(MAP)/20%LCP_1 blend (*Figure 8c*). A similar type of fibrillar morphology is observed in the PA6(MAP)/40% LCP_1 blend extruded at low and high shear rates.

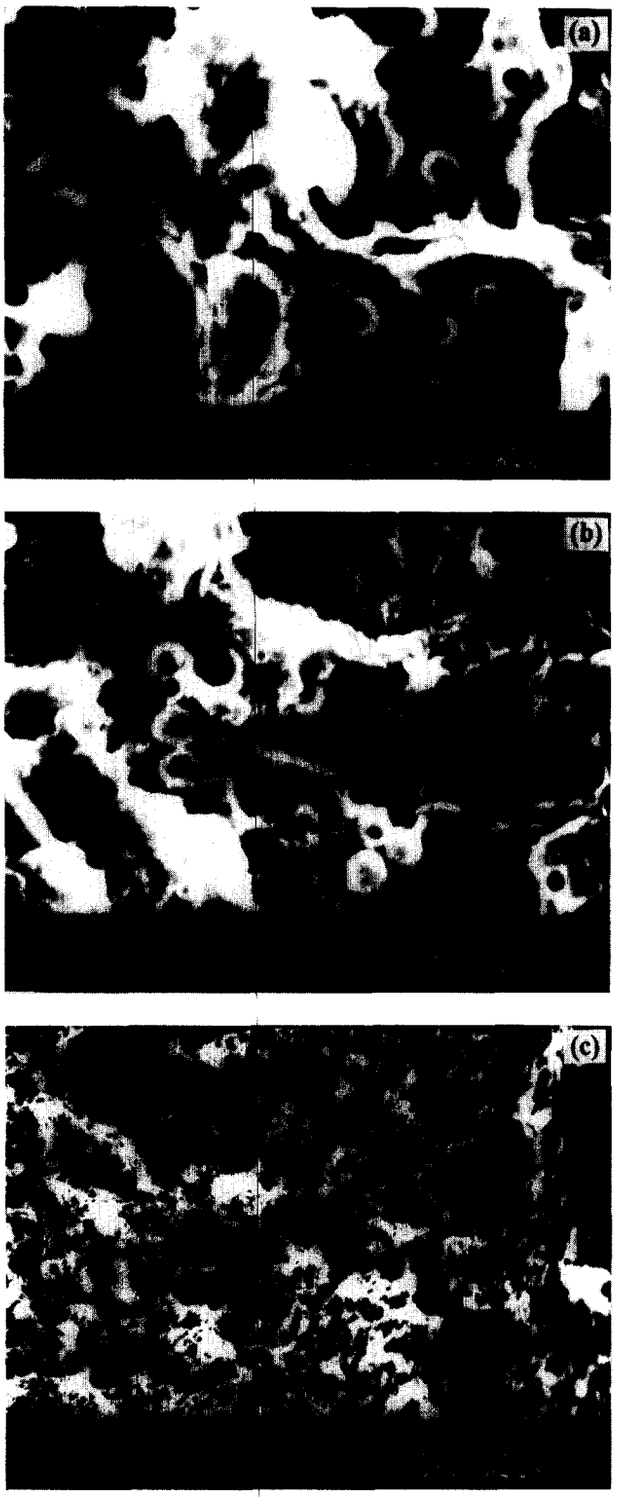

Figure 9 SEM micrographs of the PA6(MAP)LCP_2 blends containing (a) 5% LCP_2, (b) 10% LCP_2 and (c) 20% LCP_2 under a shear rate of 4883 s^{-1} at 265°C

Figure 9a–c show SEM fractographs of the PA6(MAP)/LCP_2 blends containing 5, 10 and 20 wt% LCP_2 extruded at a high shear rate of 4883 s^{-1} and at 265°C. The LCP domains appear as spherical droplets in the blend containing 5% LCP_2 whereas a distinctive foamy appearance can be seen for the blends with LCP_2 concentration $\geq$ 10%. The foamy structure is also observed in the PA6(MAP)/LCP_2 blend with 20% LCP extruded at 235°C at a high shear rate (*Figure 10*). Thus, the LCP_2 domains do not elongate into microfibrils in the polyblends with various LCP_2

Figure 10 SEM micrograph of the PA6(MAP)/LCP_2 blends containing 20% LCP_2 under a shear rate of 4883 s^{-1} at 235°C

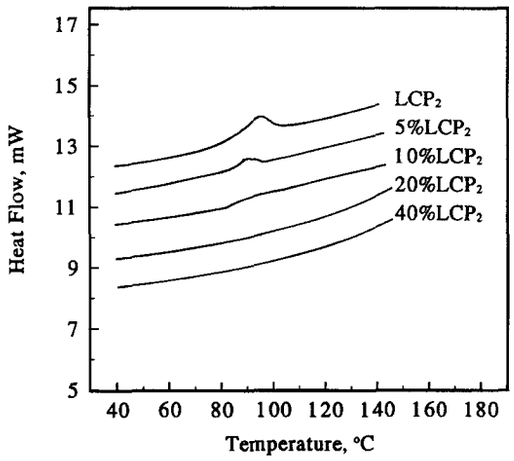

Figure 11 DSC traces of neat LCP_2 and PA6(MAP)/LCP_2 blends extruded under a shear rate of 4883 s^{-1} at 265°C

concentrations. As mentioned above, despite of the favourable rheological properties of the PA6(MAP)/LCP_2 system, no fibrillation of LCP can be produced. It is believed that the formation of porous and foamy structure in PA6(MAP)/LCP_2 blends is associated with the decomposition of PA6(MAP)/LCP_2 into substances with small molecular weight during processing. A strong decreasing trend in the viscosity of PA6(MAP)/LCP_2 blend with increasing LCP content can be attributed to the decomposition of LCP_2 and PA6(MAP) polymer during processing (*Figure 5a–b*). The thermal degradation of LCP_2 is enhanced or catalyzed by the presence of MAP copolymer. Lee and Dibenedetto[23] and Yoda *et al.*[24] reported that the LCP_2 can decompose easily into carbon dioxide and acetaldehyde, which are typical products of thermal degradation of PET. This means that LCP_2 has suffered chain scission during processing, resulting in a material of lower molecular weight[23]. It should be noted that the addition of small amount of LCP_2 is beneficial in improving the tensile strength of PP/LCP_2 blends as there are no chemical reactions take place between the LCP_2 and PP during processing[12]. *Figure 11* shows the DSC traces of neat LCP_2 and the PA6(MAP)LCP_2 blends. Apparently, the glass transition temperature (T_g) of LCP_2 is located at

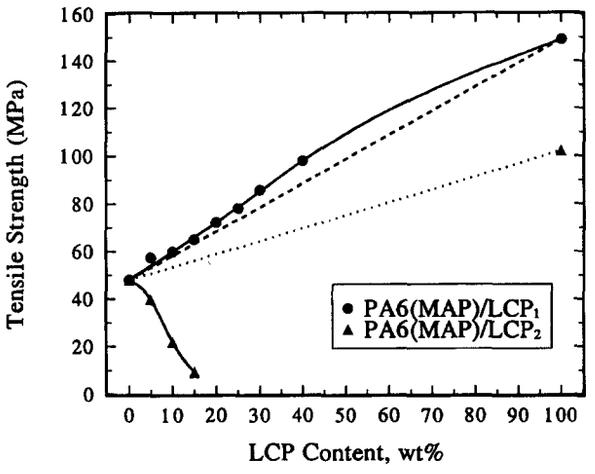

Figure 12 Variation of tensile strength with LCP content for the PA6(MAP)/LCP_1 and PA6(MAP)/LCP_2 blends. The dash lines are predicted from the rule of mixtures

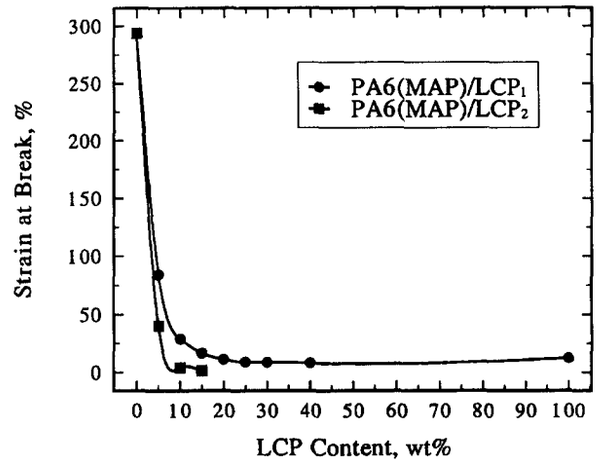

Figure 13 Variation of strain at break with LCP content for the PA6(MAP)/LCP_1 and PA6(MAP)/LCP_2 blends

about 100°C. However, the intensity of Tg decreases with increasing LCP_2 content and it disappears completely for the polyblends containing 20 wt.% LCP and above. This implies that the LCP_2 of the polyblends degrades into smaller molecules, hence its Tg becomes undetectable. Bair and co-workers reported that the LCP/PPS blends appeared foamy due to a gas that was produced by unspecified chemical reactions taking place between the two components of the blends. And, the viscosity ratio between LCP and PPS in their case favours the formation of fibrils[25,26].

Viscoelastic effect

Taylor[27] had studied the effect of the different parameters on the elongation and then on the burst of droplets in different suspensions. He showed that the deformation or bursting of spherical droplets in simple shear or elongational flow of Newtonian fluid is related to the viscosities of the suspending fluids and dispersed fluids, shear rate and interfacial tension. The critical condition for droplet breakup is

$$\left(\frac{L-B}{L+B}\right)=\frac{\eta_m * \gamma * \alpha}{\sigma}=f\frac{(\eta_d)}{(\eta_m)}=f(V_r) \qquad (1)$$

where L and B are the length and width of the dispersed droplet, α is the droplet diameter, σ is the interfacial tension, η_m is the viscosity of the suspending fluid, η_d is the viscosity of the dispersed fluid, γ is the applied shear rate and $f(V_r)$ is the function relates to viscosity ratio between the dispersed phase and suspending liquid. Equation (1) indicates that deformation and burst of droplets depends mainly on the ratio between the viscosity of the dispersion phase and the viscosity of the suspending fluid. In other words, a fibrillar morphology will occur when the V_r is smaller or close to unity. The conditions required for droplet deformation in polymer systems is more complicated owing to the fact that the polymers exhibit viscoelastic behaviour. Han has investigated the deformation of two immiscible viscoelastic fluids under shear and elongational flows, and indicated that deformation occurs more easier in an extensional flow field. Furthermore, the elasticity of viscoelastic fluids delays droplet breakup[28,29].

From *Table 1*, the viscosity ratio values between the LCP and matrix show that fibrillation of LCP fibrils in PA6(MAP)/LCP_1 system is unlikely to occur. However, SEM examinations reveal that fine fibrils are observed in this system particularly for the blends containing higher LCP concentrations and under high shear rates. The reason why the V_r values do not correlate with the resulting morphology arises from the ignorance of viscoelastic factors. It is widely recognized that long and rigid molecular chains of dispersed LCP and suspending thermoplastic plastics exhibit a large viscous force during deformation. Thus, the viscoelastic parameter must be taken into account for the non-Newtonian fluid. In this case, equation (1) is tentatively modified as follows

$$\left(\frac{L-B}{L+B}\right)=f(V_r)f(E_r) \qquad (2)$$

where $f(E_r)$ is a function of the viscoelastic ratio between the dispersed component and suspending matrix. As the $f(E_r)$ is smaller than unity, thus the product $f(V_r)\cdot f(E_r)$ becomes smaller than unity even though the $f(V_r)$ is larger than one. And, this explains the formation of LCP fibrils in PA6(MAP)/LCP_1 system with V_r values larger than one. Similarly, fibrillar morphology has been reported for PA6/LCP blends where V_r values are larger than nine[14].

Mechanical properties

Figure 12 shows the variation of tensile strength with LCP content for the PA6(MAP)/LCP blends. It can be seen that the tensile strength tends to increase with increasing LCP content for the PA6(MAP)/LCP_1 system. Furthermore, the tensile strength of the blends appears to deviate positively from the prediction of the rule of mixtures. This implies that the LCP fibrils reinforce the PA6(MAP) matrix effectively. This result is of practical importance in the LCP reinforced composites as the tensile strength of the in situ composites is generally lower than that predicted from the rule of mixtures. The enhancement in tensile properties of the PA6(MAP)/LCP_1 system can be attributed to an increase in compatibility between the LCP_1 and PA6 brought about by the addition of maleated PP. On the other hand, the tensile strength appears to decrease significantly with increasing LCP content for the PA6(MAP)/LCP_2 system. This is due to the LCP_2 phase dispersed into porous and foamy structure rather than extended fine fibrils. The strain at break vs LCP content

for the PA6(MAP)/LCP blends is shown in *Figure 13*. It is noticed that the strain at break decreases dramatically with increasing LCP content in the PA6(MAP)/LCP_1 system, and this is the typical characteristic of the polymer composites.

CONCLUSION

The results of the rheological measurements show that the steady shear viscosity of the compatibilized blends of PA6 and LCP, exhibit a complex behaviour. The fibrillation of LCP does not correlate in a simple manner with the viscosity ratio of the LCP dispersed phase to the polymer matrix and it is considered that the viscoelastic behaviour must also be taken into account during LCP fibril formation. In general, tensile test results show that the tensile strength tends to increase with increasing LCP content for the PA6(MAP)/LCP_1 system in a manner that deviates from a simple additive rule of mixtures. LCP fibrillation does not occur in the PA6(MAP)LCP_2 owing to the decomposition of LCP_2 and maleated matrix during processing and therefore, in this case, the tensile strength decreases sharply with LCP content.

REFERENCES

1. Limtasiri, T. and Isayev, A. I., *J. Appl. Polym. Sci.*, 1991, **42**, 2923.
2. Turek, D. E. and Simon, G. P., *Polymer*, 1993, **34**, 2750.
3. Lekakou, C. and Dickinson, C. E., *High Perform. Polym.*, 1996, **8**, 109.
4. Wei, K. H. and Kiss, G., *Polym. Eng. Sci.*, 1996, **36**, 713.
5. Tjong, S. C., Liu, S. L. and Li, R. K. Y., *J. Mater. Sci.*, 1995, **30**, 353.
6. Tjong, S. C., Shen, J. S. and Liu, S. L., *Polym. Eng. Sci.*, 1996, **36**, 797.
7. Tjong, S. C., Liu, S. L. and Li, R. K. Y., *J. Mater. Sci.*, 1996, **31**, 479.
8. Done, D. and Baird, D. G., *Polymer*, 1990, **30**, 989.
9. Bretas, R. E. S. and Baird, D. G., *Polymer*, 1992, **33**, 5233.
10. Datta, A., Chen, H. H. and Baird, D. G., *Polymer*, 1993, **34**, 759.
11. O'Donnell, H. J. and Baird, D. G., *Polymer*, 1995, **36**, 3113.
12. Datta, A. and Baird, D. G., *Polymer*, 1995, **36**, 505.
13. Wei, K. H., Hwang, W. J. and Tyan, H. L., *Polymer*, 1996, **37**, 2087.
14. Beery, D., Kenig, S. and Siegmann, A., *Polym. Eng. Sci.*, 1991, **31**, 451.
15. Blizard, K. G., Federici, C., Federico, O. and Chapoy, L. L., *Polym. Eng. Sci.*, 1990, **30**, 1442.
16. Mehta, A. and Isayev, A. I., *Polym. Eng. Sci.*, 1991, **31**, 971.
17. Valenza, A., Mantia, F. P., Minkova, L. I., De Petris, S., Paci, M. and Magagnini, P. L., *J. Appl. Polym. Sci.*, 1994, **52**, 1653.
18. Crevecoeur, G. and Groeninckx, G., *Polym. Eng. Sci.*, 1993, **33**, 937.
19. Subramanian, P. R. and Isayev, A. I., *Polymer*, 1991, **32**, 1961.
20. Isayev, A. I. and Subramanian, P. R., *Polym. Eng. Sci.*, 1992, **32**, 85.
21. Tjong, S.C. and Meng, Y.Z., *Polymer Int.*, 1997, **42**, 209.
22. Tjong, S. C. and Meng, Y. Z., *Polymer*, in press.
23. Lee, W. C. and Dibenedetto, A. T., *Polym. Eng. Sci.*, 1992, **32**, 400.
24. Yoda, K., Tsuboi, A., Wada, M. and Yamadera, R., *J. Appl. Polym. Sci.*, 1970, **14**, 2357.
25. Ramanathan, R., Blizzard, K. and Baird, D. G., *SPE ANTEC*, 1988, **34**, 1123.
26. Baird, D. G. and Sun, T., in *Liquid Crystalline Polymers*, ed. R. A. Weiss and C. K. Ober. American Chemical Society, Washington DC, 1990.
27. Taylor, G. I., *Proc. Roy. Soc.*, 1934, **A146**, 501.
28. Chin, H. B. and Han, D., *J. Rheol.*, 1979, **23**, 557.
29. Chin, H. B. and Han, D., *J. Rheol.*, 1980, **24**, 1.